Received: 7 November 2023 | Revised: 3 January 2024 | Accepted: 25 January 2024

DOI: 10.1002/jms.5008

Journal of MASS SPECTROMETRY WILEY

REVIEW ARTICLE

Nordic Symposium for Mass Spectrometry 2023

Spatial neurolipidomics—MALDI mass spectrometry imaging of lipids in brain pathologies

Durga Jha[1] | Kaj Blennow[1,2,3,4] | Henrik Zetterberg[1,2,5,6,7,8] | Jeffrey N. Savas[9] | Jörg Hanrieder[1,2,6]

[1]Department of Psychiatry and Neurochemistry, Institute of Neuroscience and Physiology, Sahlgrenska Academy at the University of Gothenburg, Mölndal Hospital, Mölndal, Sweden

[2]Clinical Neurochemistry Lab, Sahlgrenska University Hospital, Mölndal, Sweden

[3]Paris Brain Institute, ICM, Pitié-Salpêtrière Hospital, Sorbonne University, Paris, France

[4]Neurodegenerative Disorder Research Center, Division of Life Sciences and Medicine, Department of Neurology, Institute on Aging and Brain Disorders, University of Science and Technology of China and First Affiliated Hospital of USTC, Hefei, China

[5]UK Dementia Research Institute at UCL, London, UK

[6]Department of Neurodegenerative Disease, Queen Square Institute of Neurology, University College London, London, UK

[7]Hong Kong Center for Neurodegenerative Diseases, Clear Water Bay, Hong Kong, China

[8]Wisconsin Alzheimer's Disease Research Center, University of Wisconsin School of Medicine and Public Health, University of Wisconsin-Madison, Madison, Wisconsin, USA

[9]Department of Neurology, Northwestern University Feinberg School of Medicine, Northwestern University, Chicago, Illinois, USA

Correspondence
Jörg Hanrieder, PhD, Department of Psychiatry and Neurochemistry, Sahlgrenska Academy at the University of Gothenburg, Mölndal Hospital, House V, 431 80 Mölndal, Sweden.
Email: jh@gu.se

Funding information
European Union Joint Programme - Neurodegenerative Disease Research, Grant/Award Number: JPND2021-00694; H2020 Marie Skłodowska-Curie Actions, Grant/Award Number: 860197; National Institute for Health and Care Research; UK Dementia Research Institute at UCL, Grant/Award Number: UKDRI-1003; Bluefield Project; AD Strategic Fund and Alzheimers Association, Grant/Award Numbers: ADSF-21-831376-C, ADSF-21-831381-C, ADSF-21-831377-C; Familjen Erling-Perssons Stiftelse, Grant/Award Number: FO2022-0270; Olav Thon Stiftelsen; Alzheimerfonden, Grant/Award Numbers: AF-968238, AF-939767, AF-930351, AF-939721, AF-968270; Vetenskapsrådet, Grant/Award Numbers: 2019-02397, 2023-02796, 2023-00356, 2022-01018, 2017-00915, 2022-00732; Alzheimer's Drug Discovery

Abstract

Given the complexity of nervous tissues, understanding neurochemical pathophysiology puts high demands on bioanalytical techniques with respect to specificity and sensitivity. Mass spectrometry imaging (MSI) has evolved to become an important, biochemical imaging technology for spatial biology in biological and translational research. The technique facilitates comprehensive, sensitive elucidation of the spatial distribution patterns of drugs, lipids, peptides, and small proteins in situ. Matrix-assisted laser desorption ionization (MALDI)-based MSI is the dominating modality due to its broad applicability and fair compromise of selectivity, sensitivity price, throughput, and ease of use. This is particularly relevant for the analysis of spatial lipid patterns, where no other comparable spatial profiling tools are available. Understanding spatial lipid biology in nervous tissue is therefore a key and emerging application area of MSI research. The aim of this review is to give a concise guide through the MSI workflow for lipid imaging in central nervous system (CNS) tissues and essential parameters to consider while developing and optimizing MSI assays. Further, this review provides a broad overview of key developments and applications of MALDI MSI-based spatial neurolipidomics to map lipid dynamics in neuronal structures, ultimately contributing to a better understanding of neurodegenerative disease pathology.

Foundation; Hjärnfonden, Grant/Award Numbers: FO2022-0311, FO2017-0243, ALZ2022-0006; Åhlén-stiftelsen; Magnus Bergvalls Stiftelse, Grant/Award Number: 213027; Gun och Bertil Stohnes Stiftelse; Stiftelsen för Gamla Tjänarinnor; National Institutes of Health, Grant/Award Numbers: R01 AG078796, R21AG078538, R21AG080705, R21AG072343; Kirsten og Freddy Johansens Fond; Alzheimer's Association, Grant/Award Numbers: ZEN-21-848495, SG-23-1038904 QC; Swedish State Support for Clinical Research, Grant/Award Number: ALFGBG-71320

KEYWORDS

Alzheimer's disease (AD), amyloid, gangliosides, inositols, lysolipids, mass spectrometry imaging (MSI), matrix-assisted laser desorption ionization (MALDI), neurolipidomics, Niemann–Pick disease type C1 (NPC1), Parkinson's disease (PD), spatial biology, sphingolipids

1 | INTRODUCTION

With the increase in average life expectancy for the world's population, the prevalence of age-related diseases, including neurodegenerative diseases such as Alzheimer's disease (AD) and Parkinson's disease (PD), is also increasing. Much detail on the pathophysiological mechanisms underlying neurodegenerative disease pathology remains elusive, but mounting data point to the role of neuronal lipid species.[1–3] As much as 90% of the brain dry weight consists of lipids though the functional role of brain lipids in distinct neuropathological processes has long been underestimated. Systemically, lipid metabolism has long been known to be essential in multiple relevant metabolic and immune response mechanisms.[4–6] However, recent findings have implicated neuronal lipids in neuropathological processes beyond neuroinflammation such as neuronal signaling and amyloidogenic protein aggregation.[7–9] For instance, variations in genes encoding lipid transporter proteins mainly APOE[9–12] and lipid-sensing microglial surface receptors (e.g., TREM2)[13–15] have been associated with an increased risk of developing sporadic AD.[14] Similarly, mutations in glycolipid-processing enzymes glucocerebrosidase (GBA) are associated with both familial forms of PD[3] and lysosomal storage disorders such as Niemann–Pick disease,[16] Sandhoff disease, and Guillain–Barré syndrome.[17]

A functional understanding of how lipids modulate neuropathological processes is still just beginning to emerge, highlighting the need for further lipid-centric neuroscience research making use of novel tools such as mass spectrometry. Significant advances in our understanding of CNS-related molecular mechanisms in neurodegeneration have been made because of the development of novel, advanced, high-resolution imaging techniques.

Commonly used spatial techniques in molecular biology research include immunohistochemistry for proteins and lipids and in situ hybridization for nucleotides (DNA/RNA) that are interfaced with brightfield- and fluorescent microscopy.

The major challenge in biochemical imaging relates to chemical specificity, selectivity, and spatial resolution. This is particularly relevant for lipid detection, as this is not possible using the conventional biological imaging strategies that are used for protein- (IHC) or nucleotide (PCR, FISH) detection. Spectroscopic methods such as infrared- (IR)[18–20] or coherent anti-Stokes Raman spectroscopy (CARS)[21] are used for chemical imaging of, for example, lipid classes and their saturation across tissue sections, though do not facilitate the identification of single lipid species.

A relatively novel molecular imaging technology, mass spectrometry (MS)-based imaging (MSI),[22–25] has, over the last years, made significant inroads into biomedical research and neuroscience research, in particular.[26–30]

Due to the revolutionizing development of soft ionization techniques such as MALDI[31] and electrospray ionization (ESI),[32] mass spectrometry became the method of choice for protein characterization fueling the development of proteomics.[33] Further, MS allows fast, sensitive, and specific detection and characterization of intact large biomolecules, including lipids, peptides, and proteins. Though MS-based approaches to tissue extracts facilitate sensitive lipidomic profiling, no accurate spatial information is maintained. Due to the complexity of the CNS, the spatial information of neurochemical distribution patterns is of significant interest to delineate ongoing neuronal mechanisms.

Being a mass spectrometry technique, MSI is characterized by providing high chemical specificity at high sensitivity.[30] Due to the versatility of the detector range, MSI allows for comprehensive spatial omics profiling of either lipids, metabolites, or small proteins in a single tissue imaging experiment. This way, typically more than 100, and for dual polarity experiments, even >200 different lipid species[34] can be discerned easily at 10-μm resolution.

2 | MASS SPECTROMETRY IMAGING

Different MSI modalities have been introduced based on different means of analyte desorption and ionization from the biological sample. The most prominent MSI modalities include laser-based systems such as MALDI MSI as well as less common but complementary tools such as LA-ICP and LAESI. Another emerging MSI modality is desorption electrospray ionization (DESI).[35] Given the advantage of an atmospheric pressure interface and no requirements for sample preparation, DESI is gaining popularity in multiple research areas spanning from fieldwork to diagnostics and drug development. Surface-enhanced laser desorption/ionization (SALDI) methods offer another LDI-based MSI option with no matrix requirement while enabling imaging at high resolution with less noise.[36,37] Finally, ion beam-based techniques, that is, secondary ion mass spectrometry (SIMS),[38] are

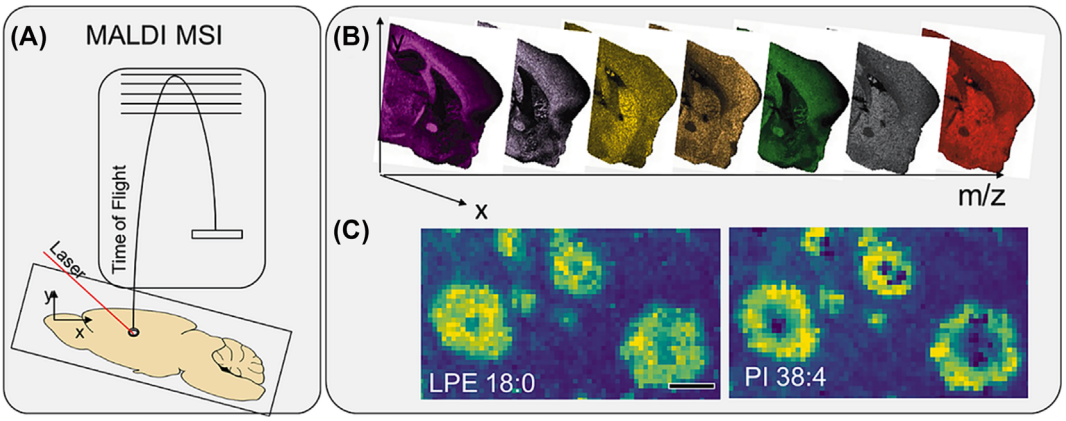

FIGURE 1 Principle of MALDI mass spectrometry imaging. (A) MALDI MS is performed in situ, where matrix-covered tissue sections are analyzed. Analyte ions are generated upon laser irradiation and transferred into a mass analyzer, for example, a time of flight. A single mass spectrum is acquired for every xi,yj coordinate of a predefined tissue array defining the image area and pixel distance. (B,C) Single ion images are generated by mapping the intensity of an individual ion signal (m/z; relative intensity) over the whole tissue slide.[42] (C) Example of MALDI MSI of transgenic AD mouse brain showing lipid localization to amyloid plaque pathology. Scalebar: 50 µm.

more and more used for biochemical imaging both for intact lipids[39] but also for proteins and protein fragments.[40,41]

The principle of MSI is based on the sequential acquisition of single mass spectra in a predefined acquisition array across a tissue section. Here, the difference between two acquisition events defines the pixel resolution. The exact spatial resolution depends on whether a discrete acquisition approach (stepwise moving stage and probe) or a scanning probe and/or a continuously moving stage is used. Aside from this consideration, the intensity distribution across the tissue array can be visualized for a given mass signal yielding single ion images (Figure 1). Different MSI technologies have various strengths and limitations, particularly regarding spatial resolution, molecular information, and mass range, respectively.

MALDI MSI represents a compromise between molecular mass range, sensitivity, and specificity. The technique is based on in situ analyte desorption and ionization upon irradiation with a UV laser. In MALDI MSI, a crystalline UV radiation-absorbing matrix is sprayed onto the tissue before laser irradiation to facilitate the desorption and ionization process.[31]

The concept of MALD MSI was demonstrated by Bernhard Spengler in 1994[25] and Richard Caprioli in 1997.[23] The main advantage of MALDI over other techniques is its mass range and selectivity, making it a versatile approach for chemical imaging of both low and high-molecular-weight species ranging from smaller drugs to complex lipids and small proteins. Aside from its versatility, MALDI is further characterized by its fair tradeoff of high resolution, specificity, sensitivity, robustness, and acquisition speed. In terms of resolution, commercial MALDI systems can achieve 5 µm. Instrumental advancements have allowed for even higher spatial resolution, such as 1.4 µm[43] with an in-house-developed highly focused MALDI source mounted onto an orbitrap system or even 0.6 µm using laser post ionization and a transmission mode instrument geometry.[44] Therefore, MALDI MSI is currently the most common MSI methodology.

Therefore, the present review focuses on MALDI MSI and aims to provide a concise overview of its application for lipid imaging in brain tissue. Here, a step-by-step guide through the experimental setup and workflow is given to enable the reader to replicate MALDI MSI experiments in-house successfully. Different advances and challenges concerning sample preparation, data acquisition, and validation are discussed. Finally, an overview of MALDI MSI-based lipid applications focusing on neurodegenerative disease pathology is provided.

3 | EXPERIMENTAL CONSIDERATIONS

3.1 | Sample preparation for MALDI imaging of lipids

For MSI-based lipid imaging, various target preparation parameters are of critical relevance as they significantly impact final data quality. This particularly concerns signal intensity, reproducibility, and lateral (i.e., spatial) resolution. The sample preparation workflow in MALDI MSI comprises tissue retrieval and storage, tissue sectioning, tissue wash, and matrix application. Tissue handling during recovery (dissection) and slice collection is critical. Similarly, matrix application facilitating sufficient analyte extraction while avoiding lateral diffusion and large crystal formation are cornerstones for each MALDI MSI experiment. These steps must be adjusted for both the type of tissue and, most importantly, the molecular target of interest.

3.1.1 | Tissue handling

For most MSI experiments, including lipid imaging, fresh frozen (FF) tissues are used due to the interference of fixation and embedding chemicals with MS analysis. Removal of those polymers is typically achieved through organic wash, which consequently would also

remove lipids. Hence, those samples do not permit the analysis of endogenous lipids due to the extensive washing for polymer removal. Therefore, FF tissue samples are preferred for MSI. To ensure the appropriate quality of FF tissue, tissue retrieval, and storage are essential. Starting with sample retrieval, typically a short post-mortem delay until dissection, collection, and processing (freezing) is critical to minimize analyte degradation.[45,46] Dissected fresh tissue samples are typically snap-frozen on dry ice or liquid propane or nitrogen and stored at −80°C.

3.1.2 | Tissue sectioning

One of the first and crucial steps in the MALDI MSI workflow is tissue sectioning. The tools and objects should be cooled to the operating temperature of −20°C. Tissues should be transported in a closed container on dry ice and allowed to acclimatize. The cryotome chamber needs to be surface sterilized with a disinfectant like ethanol. The tissue is mounted to the cryostat chuck by placing a small drop of embedding media (e.g., optimal cutting temperature [OCT] compound), putting the chuck into the cooling chamber of the cryostat and holding the tissue piece onto the mounting medium with ice-cold tweezers while the mounting medium freezes. In contrast to cryosectioning protocols used in pathology and histology, tissues cannot be immersed/embedded in OCT for cutting, and contamination with OCT of the cutting surface of the tissue, the cryo-collection table, or the blade must be avoided at all costs.

The OCT compound should be allowed to solidify at −20°C. The tissue-mounted chuck is then attached to the holder, and sectioning can begin with a thickness of 12 μm. The sections can be transferred onto a glass slide using a brush. Finally, the tissue can be thawed by warming the glass slide from underneath with a finger. It is essential to ensure that the tissue is completely thawed before proceeding with any further staining or analysis. Thawing the tissue too quickly or unevenly can lead to damage and loss of cellular integrity. Therefore, allowing the tissue to thaw at room temperature for sufficient time is recommended before continuing with the desired protocol. It is important to note that the operating temperature and blade condition can affect the outcome, and precautions should be taken to avoid humidity in the chamber. To ensure optimal results, it is recommended to maintain a controlled environment with low humidity during the sectioning process. Additionally, the blade should be regularly held and sharpened to achieve clean and precise sections. Following tissue sectioning, the composed sections must be dried in a desiccator for 10 min before storage at −80°C to prevent damage by water condensation during freezing.[47]

3.1.3 | Tissue washing and matrix application

One of the biggest sources of interference is tissue preparation. This step involves the thawing and washing of the stored cryosections and subsequent matrix application. The initial washings are used to remove contaminants and salts. In the case of lipid imaging, this step involves washes with ammonium salts,[48,49] while peptide and protein analysis involves organic washes or organic wash accompanied by buffer wash for lipid removal and protein precipitation.[50,51] Matrix application can be performed using different approaches of deposition and roughly be divided into three categories: (a) nebulizer/sprayer, (b) microspotting, and (c) sublimation.

The application methods are chosen concerning the analyte targeted, spatial resolution, reproducibility, and sensitivity. Desorption and ionization of charged lipid molecules are easily achievable due to their high abundance. Matrix-free, surface-assisted LDI methods have been reported to accomplish this task using functional surfaces such as DIOS,[52] NIMS,[37] or Si-nanorods.[53,54] These methods are superior concerning spatial resolution and sample handling. However, they have limitations regarding tissue preparation (sectioning), requiring very thin tissue sections along with sensitivity and reproducibility issues. Consequently, matrix-assisted LDI is more prominent, given the rather straightforward sample preparation, increased sensitivity, range of analytes, and robustness.

The most used approach involves matrix spraying using commercially available robotic nebulizer-assisted pneumatic sprayer systems, such as the TM or M3 + Sprayer (HTX Technologies), SunCollect Sprayer (Sunchrom), or iMLayer (Shimadzu), along with open-source or even manual airbrush systems.

Potential sources of error during matrix application include the matrix solvent being too dry or too wet, which could result in solvent evaporation or analyte diffusion; thus, there is a need to be observant for leaks and clogging during runs. To overcome these challenges, other approaches, such as using a heated spray head (HTX Sprayers), dry coating,[55] or matrix sublimation,[56–58] have been introduced allowing for control crystal size.[55,57] While sublimation provides significant advantages in terms of crystal size, the earlier approach had limitations concerning repeatability and extraction efficiency; however, recent developments make matrix sublimation a potent alternative for lipid analysis.[59]

Different matrices have been proposed for MALDI MSI of various molecular species, including other lipids varying in polarity and hydrophobicity. For lipid analysis, the most used matrices are 2,5-dihydroxy-benzoic acid (DHB),[60] 1,5 di-amino-naphthalene (1,5-DAN),[56] norharmane,[61] 9-aminoacridine (9-AA),[62] N-(1-naphthyl) ethylenediamine (NEDC),[63] and 4-hydroxyl-alpha-cyano-cinnaminic acid (CHCA). The choice of the matrix depends on the targeted analyte class, crystal size, mass range, and matrix cluster formation.

3.2 | MALDI mass spectrometry experimental

3.2.1 | MALDI MSI instrumentation

Several MALDI MSI solutions are commercially available. Generally, MALDI MSI instruments can be divided into high vacuum MALDI ToF systems and medium pressure/atmospheric pressure (AP) MALDI setups, where a MALDI ion source is mounted onto an otherwise ESI MS setup.

MALDI ToF systems such as Shimadzu's Axima, 8030, and 7090 as well as Bruker's rapifleX/ultrafleXtreme provide very high sensitivity and acquisition speed and have advantages in terms of mass range, for example, endogenous peptide analysis. Limitations of those setups lie with mass resolution, particularly for compounds over m/z 6000 that are analyzed in linear mode, the complexity of the systems with a high vacuum source, and MS/MS analysis typically relying on post-source decay with ion gate-based precursor ion selection. This approach has limitations with respect to precursor ion selection by flight time and, particularly for smaller molecules, and fragmentation efficiency resulting in lower MS/MS sensitivity while consuming samples due to increased laser power. Those challenges have been addressed by including collision chambers or ion traps for CID/CAD fragmentation as found in both Bruker's and Shimadzus' MALDI ToF systems, along with MS^n capabilities warranted by the ion trap (IT) in the Axima QIT-ToF systems.[64] A limitation of MALDI-ToF systems is mass resolution, which is typically limited to 40 000 in reflector mode, and which makes it difficult to discern low molecular weight species from matrix signals. This is overcome in more exotic systems such as the Jeol Spiral ToF,[65,66] or SimulToF,[67] which allow obtaining mass resolution of 50 000 (SimulToF) up to 100 000 (SpiralToF).

AP or medium-pressure MALDI MS systems bring together the advantages of MALDI MSI in terms of spatial resolution with higher mass resolution (>40 000) and more complex mass analyzers including ToF (Shimadzu iMScope[68] and Waters Synapt) or FT analyzers such as Bruker's SolariX and ScimaX FTICR MS and Thermo MALDI-orbitrap equipped with an intermediate pressure MALDI source.[43,69] Further, ion mobility-ToF hybrid analyzers (Bruker TIMS ToF flex, Waters Synapt IMS/cyclic IMS) are available, which are particularly beneficial for resolving isomers in lipid analysis.[20,70–73] AP or medium-pressure MALDI MSI systems have limitations in, for example, terms of sensitivity toward higher molecular weight compounds (peptides and proteins) but offer significant advantages for characterizing and quantifying smaller molecules (lipids) because those systems offer higher mass accuracy, ion mobility, and superior MS/MS or MS^n capabilities. For MALDI-FTICR and MALDI-orbitrap MSI, some challenges remain with respect to scan speed to the benefit of superior mass resolution.

3.2.2 | MALDI MSI data acquisition

The parameters for a MALDI imaging experiment are typically specified in an acquisition sequence, specified in the respective MS imaging software. Here, all the acquisition and initial data processing parameters are specified along with the acquisition region, acquisition pattern, and spot-to-spot distance, that is, spatial resolution. The initial steps of setting up the imaging acquisition experiment involve image registration and teaching for sequence setup, performed in the imaging software provided by the vendor.

For the actual MALDI acquisition method, the optimum number of good-quality spectra that can be obtained from each position must be specified, including the number of laser shots and laser intensity (i.e., fluence). Too high laser fluence can influence the experiment dramatically, leading to signal depletion due to oversampling effects.[74] Here, the spatial resolution and laser focus settings must be considered accordingly, as small spot-to-spot distances at too high laser fluence lead to the described oversampling phenomena. For a typical DHB or DAN matrix for lipid analysis, five to 10 shots at lower energies are needed to allow straightforward acquisition of imaging data at 10 µm.[74] When specifying the pixel distance and spatial resolution, a further consideration is the acquisition time. Assuming a MALDI instrument with a 10-kHz laser is used, acquiring extensive areas at very high spatial resolution will take several hours. During this time, the matrix might sublimate away, making it impossible to acquire reliable data.

Another critical factor to consider during data acquisition is the external calibration of the instrument before sample analysis to ensure accurate and reliable lipid identification. In lipid MALDI MSI experiments, some of the routine external calibrants used are red phosphorus,[75–77] a mixture of standard peptides,[56,75–81] or a mix of lipid standards[82,83] (Table 1). It is always mandatory to include at least two calibration spots placed in two corners diametrically over the slide and save the spectra to go back later and recalibrate.

3.3 | Data analysis

3.3.1 | Data processing

Imaging data acquisition is generally followed by data processing, including baseline subtraction, peak picking, and calibration. On-the-fly MS processing uses a baseline removal algorithm that will not result in negative data (e.g., ConvexHull 0.8 flatness; FlexAnalysis, Bruker Daltonics). Peak picking is performed using sensitive algorithms (Centroid, SNAP) considering peaks with a minimum signal-to-noise (S/N) > 3. There are several tools for data analysis for MSI, such as Flex Analysis (Bruker), Image Reveal (Shimadzu), High Definition Imaging (HDI, Waters), and ImageQuest (Thermo Fisher Scientific, Massachusetts, USA) as well as commercial and free-standing, vendor-independent options such as Lipostar,[85] SCiLS (Bruker), Mozaic (Spectroswiss, Lausanne, Switzerland), MALDIVision, MSiReader,[86] Cardinal,[87] Biomap,[88] msiQuant,[89] and SpectralAnalysis.[90]

3.3.2 | Statistical analysis

The complexity of high-content MALDI MSI data poses a significant challenge for data analysis. High-resolution imaging data can result in multiple gigabyte file sizes that for comparative/multimodal analysis of multiple datasets easily exceed the computational power of standard systems and highlight the need to balance imaging area, mass range, and spatial resolution. A typical MSI data analysis workflow involves three steps: (1) segmentation and region of interest (ROI) identification, (2) ROI spectral analysis, and finally (3) univariate analysis.

TABLE 1 Example of routinely used external calibrants for lipid analysis through MALDI-IMS. 2,5-Dihydroxybenzoic acid (DHB), sinapinic acid (SA), α-cyano-4-hydroxycinnamic acid (CHCA), N-naphthylethylenediamine dihydrochloride (NEDC), 2′,4′,6′-trihydroxyacetophenone monohydrate (THAP), 1,5-diaminonaphthalene (DAN).

Study	External calibrants	Matrix	Tissue	Instrument
Kaya et al.[76]	Red phosphorus	Norharmane	Non-human primate coronal brain	MALDI-FTICR (SolariX, Bruker)
Angelini et al.[83]	A mixture of phosphatidylcholine and lysophosphatidylcholine	CHCA	Mouse brain	MALDI TOF/TOF (UltraFlextreme, Bruker)
Liang et al.[81]	A mixture of DHB, SA, CHCA, and peptides.	NEDC	Whole zebrafish	MALDI-TOF/TOF (RapifleX, Bruker)
Tobias et al.[77]	Red phosphorus	9AA (lipids) DHB (Cholesterol)	Mouse brain	MALDI TOF/TOF (Sciex)
Kaya et al.[84]	A mixture of standard peptides	DAN	Mouse brain	MALDI TOF/TOF (UltraFlextreme, Bruker)
Mallah et al.[80]	A mixture of standard peptides	DHB	Rat brain	MALDI-LTQ-Orbitrap-XL (Thermo Fisher Scientific)
Prentice et al.[78]	A mixture of standard peptides for positive mode calibration and matrix clusters for negative mode calibration	DAN	Mouse brain	MALDI TOF/TOF In-house built
O'Rourke et al.[75]	Red Phosphorus	DHB	Human brain	MALDI TOF/TOF (UltraFlextreme, Bruker)
Jackson et al.[82]	A mixture of phosphatidylcholines and sphingomyelins	DHA	Rat brain	MALDI-TOF/TOF (Applied Biosystems)
Thomas et al.[56]	Lipid and peptide mixture	DAN	Mouse brain, liver Fish whole body	MALDI TOF/TOF (UltraFlextreme, Bruker)

To approach the entire MSI dataset, the first step involves a reduction in dimensionality using multivariate data analysis (MVDA) tools such as principal component analysis (PCA),[91] maximum autocorrelation factor analysis (MAF),[29] hierarchical cluster analysis/bisecting k-means clustering,[91,92] and orthogonal projections on latent structure analysis (OPLS).[42,91] The aim is to reduce data complexity and capture tissue heterogeneity encoded in covariate patterns of individual chemical species in discrete MVDA factors (e.g., principal components) or clusters, respectively. The goal is then to annotate distinct histological features that are captured into the same MVDA factor and cluster based on their chemical similarity which is reflected in either covariance (PCA) or proximity (HCA). From the corresponding scores and loadings, the variables contributing the most (i.e., mass peak values) to these variances can be deduced, revealing histology-associated chemical changes that allow annotation of the ROI. These ROIs can further be annotated based on immunohistochemical staining subsequently performed on the same tissue section.[91] This approach serves also as a means of validation for the MVDA-based image segmentation.

The annotated regions of interest can the further investigated through both supervised and unsupervised MVDA tools such as PCA, HCA, soft independent modeling by class analogy (SIMCA), orthogonal partial least square (OPLS), multiblock OPLS (OnPLS), and OPLS discriminant analysis (OPLS-DA) for either classification or discriminative analysis.[42,91] Ultimately, univariate tools such as group comparisons (e.g., ANOVA, *t*-statistics, and Mann Whitney) or regression modeling (linear and logarithmic) can be used to validate the segmentation and MVDA data as well as verify the histological relevance of the identified chemical localization patterns.

3.4 | Lipid identification

While MSI is a very powerful approach for in situ lipid profiling, there is a need for complementary validation strategies to fully exploit the potential of the technique. Like protein and peptide imaging, initial mass peak annotation is based on accurate mass and reference values reported in the literature or online depositories, such as the LIPID MAPS,[93] Metaspace,[93] and SwissLipids Knowledgebase.[94,95] A strong advantage in the case of imaging of low molecular weight compounds, such as lipids, is the resolving power of high-end mass analyzers in that mass range, particularly Fourier transform (FT) instruments, but

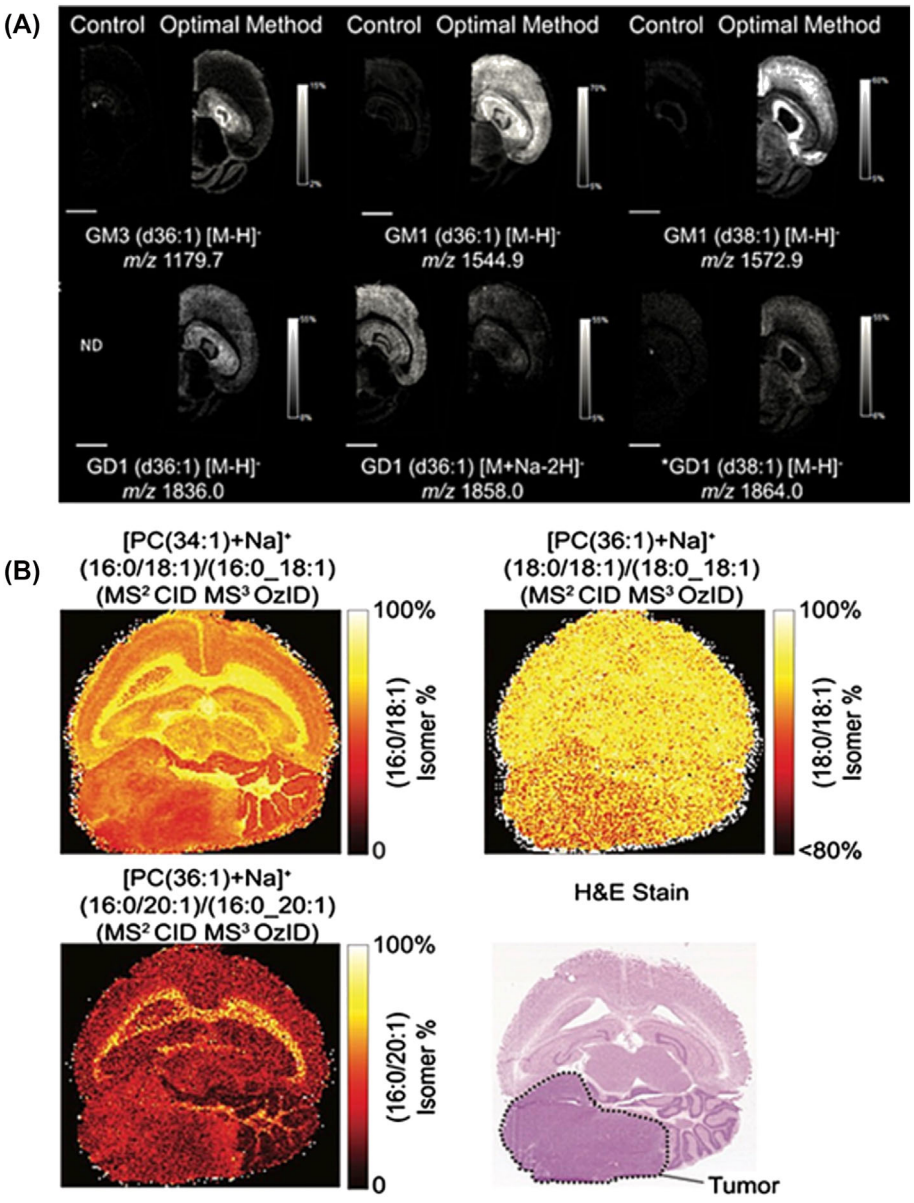

FIGURE 2 Sample preparation optimization for ganglioside analysis through MALDI-TOF MSI of mouse brain tissue sections. (A) Optimization by washing tissue sections with ammonium formate, deposition, matrix sublimation, and waiting before analysis increased ganglioside species signal intensity. Different species and fatty acyl chain lengths of gangliosides can be identified, expanding the range of complex lipids that can be studied. The scale bar is 2 mm, and the lateral resolution is 65 µm. ND: not detected. The figure has been adapted from Yang et al.[103] (B) Application of ozone-induced dissociation (OzID) in resolving double-bond (db) positional isomers. MALDI-CID/OzID fractional images of PC(16:0/18:1), PC(18:0/18:1), and PC(16:0/20:1) in an animal model of medulloblastoma. The images highlight the importance of resolving structural isomers since their distribution is specific, and heterogeneous distributions can be present even for lipids with the same fatty acyl chain, revealing pertinent information regarding disease pathogenesis.[102]

also reflector ToF analyzers. This facilitates compound identification based on low to sub-ppm mass accuracy and the elemental composition deduced by the resolved true isotope pattern. Increased confidence in identification is achieved by follow-up MS/MS or MS^n fragmentation analysis and structural characterization.[82] However, regarding MS/MS, in contrast to protein identification, this step is more challenging as lipids compounds, and their fragmentation patterns are far more diverse. This renders the generation of reference databases, such as those available for protein sequences, very challenging. Notable attempts to generate MS/MS spectral libraries have been made to address this issue but are limited due to the vast number of diverse lipid classes and species.[95,96]

A further significant challenge in lipid characterization is the identification of lipid isomers. This concerns the identification of both structural isomers and stereoisomers.[97] This is one of the most significant challenges, as isomeric lipid species can have entirely different biological functions. Very elegant approaches by in vitro and even in situ derivatization have been proposed.[98–101] Most notably, methods using gas phase ozonolysis in lipidomics and, most recently, online within an imaging experiment have been presented[98,102] (Figure 2). Similarly, an approach using in situ modification via a Paterno–Büchi reaction has been reported for localizing double bonds in isomeric phospholipids and glycolipids.[99,101]

Ion mobility MS (IM-MS) presents another compelling method for identifying various lipid classes and structural isomers.[70] The utilization of matrix-assisted laser desorption/ionization trapped ion mobility spectrometry time-of-flight-based mass spectrometry imaging (MALDI TIMS TOF MSI) in lipid identification has been a significant endeavor, as it has enhanced the reliability of correctly identifying lipids by including additional physical factors such as collisional cross-section (CCS) with improved mass accuracy.[72] This further allows identification by comparing with ex-situ lipidomic data acquired

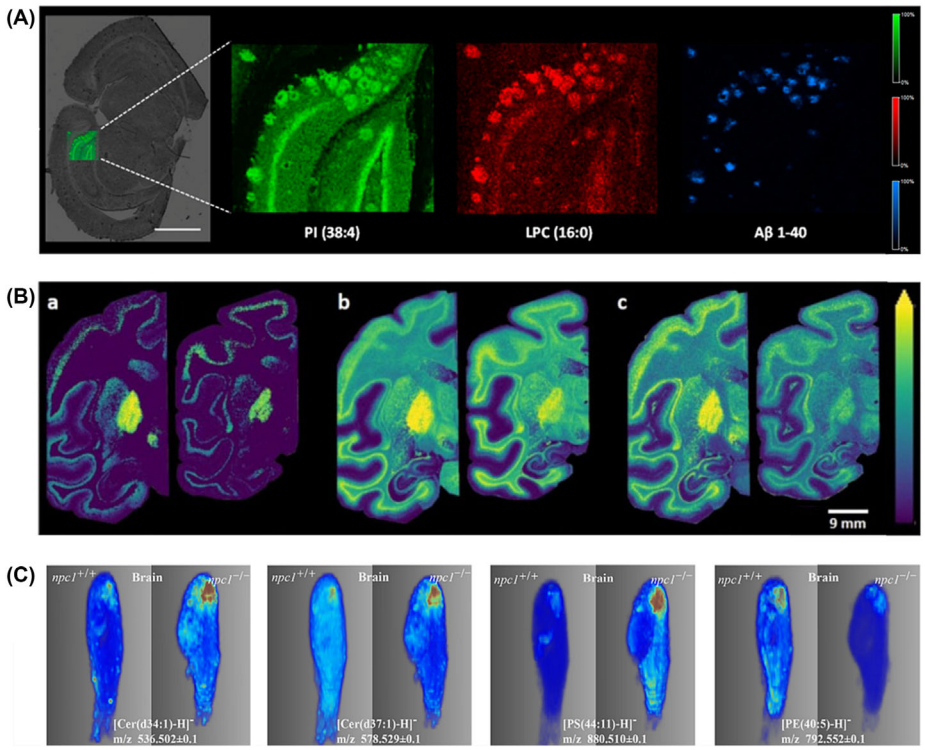

FIGURE 3 MALDI imaging of lipid species in central nervous system (CNS) tissues in different neurodegenerative diseases. (A) Multimodal MALDI-MSI revealed amyloid plaque-associated lipids in dual polarity and peptides on a coronal mice brain tissue section of transgenic Alzheimer's disease mice (tgArcSwe). Ion images of lipids obtained at 10-µm spatial resolution: phosphatidylinositols (PI 38:4, m/z 885.6) in negative (green), lysophosphatidylcholines (LPC 16:0, m/z 496.3,) in positive (red) polarities with subsequent amyloid-β (Aβ 1–40, m/z 4257.6) peptide (blue) ion images in the same imaging region.[109] (B) MALDI-MS ion images of sulfatide species (a) SHexCer (41:2), (b) SHexCer (42:2), and (c) SHexCer (42:3) in control (left) and MPTP-lesioned macaque brain tissue, a Parkinson's disease animal model. The lateral resolution is 150 µm.[76] (C) Representative 3D images of lipid in the CNS of a zebrafish model of Niemann–Pick disease 1. The 3D image was prepared by reconstructing 20 consecutive sections of a sample. The lipids shown here are ceramide (Cer 34:1, Cer 37:1), phosphatidylserine (PS 44:11), and phosphatidylethanolamine (PE 40:5). MALDI MSI was obtained in negative ion mode at a spatial resolution of 50 µm.[81]

through LC-IM-MS.[72] Together, these advances indicate that lipid characterization, in vitro and in situ, is becoming increasingly robust and routine.

4 | MALDI MSI OF NEURONAL LIPIDS IN CNS DISEASES

4.1 | Neurodegenerative diseases

Lipid analyses are relevant in neuroscience research as they have significant roles as both signaling molecules and structural interactions with membrane proteins. Moreover, it has been established that (membrane) lipids interact with self-aggregating proteins such as amyloidogenic proteins and even promote aggregation of these proteins in a pathological context. This is of relevance as abnormal aggregation and deposition of proteins is a seminal pathological hallmark in many neurodegenerative diseases, including AD, PD, Huntington's disease, amyotrophic lateral sclerosis, frontotemporal lobe dementia, and Niemann–Pick disease.

MALDI imaging offers the unique opportunity to characterize the protein pathology associated with lipid biochemistry, which in turn provides targets for mechanistic investigations.

In this context, MALDI imaging has been most prominent for delineating amyloid plaque pathology associated with lipid regulations in AD. Specifically, MALDI imaging identified plaque-specific localizations of gangliosides, ceramide, lysophosphatidic acids, and inositol; sulfatides were depleted at plaques.[104–106] Moreover, when interfaced with advanced fluorescent microscopy using structure-sensitive luminescent probes, MALDI MSI revealed amyloid polymorphism-specific lipid changes in transgenic AD mice.[107,108] Here, ganglioside GM1 correlated with the core structure of senile plaques, while ceramides and phosphoinositols were located in the diffuse periphery.[108]

Further development toward multimodal imaging approaches includes bimodal,[107,108] trimodal[109,110] lipids, and peptide imaging from the same tissue section. The low laser desorption energies facilitate this approach, fluences, and shot numbers necessary to obtain satisfactory lipid spectra using 1,5-DAN matrix dry coating protocols or sublimation.[74,109] This approach eventually allows correlating in situ lipid changes to associated protein mechanisms

identified with MSI, spectroscopy, and conventional microscopy techniques.[107,111] In detail, distinct lipids such as ganglioside GM1 were found to correlate with Aβ1–40 within spectroscopy-assigned core structures[109] (Figure 3A). In contrast, other lipids, including ceramides and inositols observed in negative mode and lysophosphocholine (LPC) detected in positive mode, correlate with diffuse parts and Aβ1–42, respectively.[112] Amyotrophic lateral sclerosis (ALS) is a fatal neurological disorder for which early diagnosis has remained elusive. A study on mouse models of familial ALS demonstrated a notable alteration in docosahexaenoic acid (DHA) distribution pattern containing PCs within the spinal cord. This shift became apparent during the terminal stage of the disease.[113] In a separate investigation employing *Drosophila melanogaster* as a model, alterations in brain phospholipid concentrations throughout the entire disease progression, commencing from the initial stages, were detected, suggesting the possibility of their utility as early biomarkers for the disease.[114] Understanding the role of lipids in ALS has remained obscure. Nonetheless, the studies mentioned above have shed light on the substantial involvement of lipids, highlighting the potential of utilizing MSI to identify potential biomarkers for early diagnosis or therapeutic targets for ALS.

Lipids are crucial to regeneration and inflammation, making them possible indicators for traumatic brain injury (TBI). High-resolution mass spectrometry revealed similar levels of palmitoylcarnitine within substantial nigra compared with the injury site. Because TBI is a risk factor for PD, the change in carnitines may suggest a pathophysiological relationship between TBI and PD, characterized by dopaminergic neuronal death.[80]

PD pathology can also be mimicked through intracranial injections of neurotoxins that induce cell death of dopaminergic midbrain neurons. Toxins like 6-hydroxy-dopamine (6-OHDA) and 1-methyl-4-phenyl-1,2,3,6-tetrahydropyridine (MPTP), are commonly utilized as a neurotoxin in monkeys and mice to simulate PD pathology[115,116] as well as for mimicing side effects for dopamine replacement therapy.[27] Here, MALDI- FTICR -MSI in dual polarity of MPTP-treated macaque monkeys found depletion of long-chain hydroxylated sulfatides in motor-related gray matter regions, suggesting myelin sheath disruption around neuron axons, which could negatively affect neural conduction and cause PD[76] (Figure 3B).

4.2 | Lysosomal storage disorders

Another neurodegenerative example where MSI can provide valuable insight is Niemann–Pick disease type C1 (NPC1), an autosomal recessive neurodegenerative disorder affecting lysosomal storage and trafficking. It is characterized by a mutation in the lysosomal transmembrane protein NPC1, responsible for most (95%) cases, which leads to dysregulation in the transport and metabolization of cholesterol and glycosphingolipids in the endosome and lysosome, resulting in cellular death. NPC1 patients typically demonstrate progressive neurodegeneration characterized by pronounced impairment of the cerebellum.[16] MSI can aid in diagnosing and monitoring the progression of NPC1 disease by accurately measuring lipid levels and their distribution in different brain regions.

In a mouse model of NPC1 study, elevated distributions of GM1, GM2, and GM3 were observed in the cerebellar region. These lipids play crucial roles in cell membrane structure and signaling pathways in the nervous system. The abnormal accumulation of these lipids in the cerebellum suggests dysregulation in lipid metabolism and potentially contributes to the progressive neurodegeneration observed in NPC1 patients. It is worth noting that the authors also disclosed a region-dependent distribution of GM2 and GM3 associated with disease progression.[77] They also observed lower amounts of GM1, HexCer, and Cer in the same region with the same fatty acid backbone (d36:1). This observation prompted them to hypothesize that the elevated levels of GM2 and GM3 were a result of the degradation of GM1. Additionally, a decrease in sulfatide levels at later time points, indicative of demyelination, was seen. They also identified a novel association between ceramide accumulation and the neurodegeneration of Purkinje cells in the cerebellum. The researchers postulated that this alteration may induce cellular death by activating cathepsin D. A marginal increase in unesterified cholesterol levels was seen in the control samples relative to the mutant mice. This observation can be attributed to the relatively lower presence of myelin in NPC1.[117]

It is important to note that imaging MS methods have limitations in accurately quantifying certain lipid species, such as cholesterol and other sterols, because of poor ionization. A study used a new derivatization method and MSI to make the process more sensitive and allow exact quantitation of sterols on sections of the whole mouse brain. Apart from the cerebellum, they also identified a significant reduction in cholesterol in the hypothalamus, midbrain, and pons in the mutant mouse compared with controls.[83] A comprehensive list of MALDI MSI for steroid and specifically cholesterol lipid analysis has been provided in Table 2.

Another pioneering study described three-dimensional MALDI MSI on the whole body of a zebrafish NPC1 model to map lipid dysregulation across different organs. Their 3D MSI displayed elevated levels of ceramide (Cer) in the brain and increased levels of sphingomyelin (SM) species in the spinal cord, where ceramide is both a precursor and degradation product of sphingomyelin, highlighting Cer-SM pathway dysregulation through the CNS[81] (Figure 3C).

4.3 | MALDI MSI of neuronal lipids in brain tumors

Given the pronounced tissue heterogeneity, MSI is a powerful technology to interrogate tumor formation and growth mechanisms and cellular cancer biology in general. The widespread presence and vital role of lipids in the CNS have spurred investigations into their involvement in the analysis of brain cancer. The heightened aerobic glycolysis of tumor cells alters lipid metabolism, rendering tumor cells and their lipid patterns a potential diagnostic and theragnostic in situ target. Consequently, MALDI MSI has been employed in various studies to evaluate the relevance of lipids in distinguishing between different types of brain tumors. In a study graft model of human glioblastoma

TABLE 2 Strategies for steroid lipid analysis through MALDI MSI.

Study	Cholesterol analysis method	Matrix	Tissue	Instrument
Angelini et al.[83]	Enzyme-assisted derivatization for sterol analysis (EADSA) 1. Conversion of the 3β-hydroxy group in cholesterol (m/z 386.3543) to 3β-oxo using cholesterol oxidase. 2. Charge tagging with Girard-P (GP) hydrazine–cholesterol hydrazone (m/z 518.4105).	CHCA	Mouse brain	MALDI TOF/TOF (UltraFlextreme, Bruker)
Barre et al.[118]	MALDI-2, a positionization strategy, was used to enable a second ionization event to increase the yield of ions. Dehydrated cholesterol (m/z 369.3521 $[M + H - H_2O]^+$)	DHB	Human cartilage and dog liver	Orbitrap elite MS coupled to an intermediate pressure MALDI/ESI interface
Dufresne et al.[119]	Silver cationized cholesterol $[M + Ag]^+$ (m/z 493–495)	Matrix free	Mouse brain/kidney	MALDI TOF/TOF (UltraFlextreme, Bruker)
Tobias et al.[77]	Unesterified cholesterol (dehydrated ion, m/z 369.3, $[M - H2O + H]^+$)	DHB	Mouse brain	MALDI TOF/TOF (ScieX)
Patti et al.[120]	Silver cationized cholesterol $[M + Ag]^+$ (m/z 493) Nanostructure initiator mass spectrometry (NIMS) combined with Silver nitrate (AgNO3)	Matrix free	Mouse brain	MALDI TOF/TOF (Applied Biosystems)
Cobice et al.[121]	7-Ketocholesterol. Charge tagging with Girard-T (GP) hydrazine precoated on the ITO slide.	CHCA	Rat adrenal gland/ mouse brain	MALDI-FTICR-MS (Bruker SolariX)
Muller et al.[122]	Silver nanoparticles implantation on tissue $[M + Ag_3]^+$. Silver adducts of cholesterol and cholesterol ester $[M + Ag]^+$.	Matrix free	Rat brain	MALDI LTQ-XL-Orbitrap (Thermo Fisher Scientific)
Nezhad et al.[123]	Silver-assisted laser desorption ionization mass spectrometry imaging (AgLDI MSI) for cholesterol quantitation (m/z 493.26) $[^{12}CHO + {}^{107}Ag]^+$	Matrix free	Mouse brain	MALDI TOF/TOF (UltraFlextreme, Bruker)

(GBM) and medulloblastoma (MB) in rats, diminished levels of complex gangliosides, GM1 and GD1, were observed in glioma. Conversely, GM3, a less complex ganglioside, exhibited exclusive upregulation in rat glioma. In turn, GM2 was upregulated in medulloblastoma, facilitating differentiation between these two forms of brain cancer.[124] Another investigation utilized high-spatial resolution MALDI MSI to scrutinize the metabolic profiles of medulloblastoma and pineoblastoma (PB) tumors. The study identified upregulated glycerophosphoglycerols (PG) and glycerophosphocholines (PC) in MB, while sphingolipids such as the cerebroside hexosylceramide (HexCer [36:2]) as well as ceramide-1-phosphate (CerP [47:2]) were specifically upregulated in PB.[125] A study employing 3D MALDI TOF MSI on pediatric brain tumors found that metastasizing tumors exhibited distinct lipid profiles compared with nonmetastasizing tumors. A prevalent characteristic in metastasizing tumors was the reduction of lipids with an 18:1 fatty acyl chain configuration. Among the lipids elevated in metastasizing primary tumors were phosphatidylinositol (PI) and the two phosphoinositide phosphates PIP and PIP2. This indicates dysregulation of the PI3K signaling pathway, which is often attributed to alterations in the phosphatase and tensin homolog (PTEN) gene, and has in turn been linked to oncogenesis in humans due to uncontrolled cell growth and proliferation.[126]

MALDI MSI also contributes to a deeper understanding of the role of lipids in tumor initiation and progression. Here, a study in human glioblastoma multiform (GBM) tissues observed reduced levels of ω-6 fatty acids, including arachidonic acid and adrenic acid, crucial energy sources, in glioma cells compared with peritumoral tissue.[127] Another study in a GBM animal model, MALDI FTICR-based MSI revealed elevated levels of small-chain fatty acids, such as palmitic acid, linoleic acid, and PI, aligning with the malignant nature of glioma.[128]

Beyond fatty acids, critical membrane lipids have been identified as dysregulated in mouse models of glioma, particularly phospholipids and sphingolipids. Here, a decrease in common PCs, such as PC 16:0/16:0 and PC 16:0/18:0, was observed in tumor parenchyma and a heterogeneous increase of PC 16:0/16:1, PC 16:0/18:1, and PC 16:0/18:2 in the tumor tissue itself. The surge in desaturated fatty acids in tumor phospholipids has been suggested to potentially modulate tumorigenic signaling pathways and enhance tumor cell survival. Additionally, MALDI MSI results disclosed a significant reduction in tumoral sphingomyelin (SM d18:1/18:0).[129]

Efforts have also been made to integrate the MALDI MSI approach with MRI, a standard in vivo imaging tool for cancer diagnostics. A study combining in vivo MRI data with high-spectral resolution MALDI MSI from a mouse brain model of GBM revealed an upregulated, co-localized distribution of PCs and cholesterol.[130] Another technological advancement of MALDI MSI involves the integration of stable isotope tracers with MSI to investigate the flux of the metabolic landscape in brains with glioblastoma. In detail, the authors introduced an approach known as Spatial Isotopologue Spectral Analysis (SISA) to assess fatty acid synthesis and elongation flux. SISA unveiled an eightfold higher difference in palmitate elongation flux in tumor tissue compared with healthy brain tissue, possibly due to the elevated demand for 18 carbon acyl chains due to their prevalence in the membrane bilayer. This study emphasizes the potential of lipid synthesis as a promising therapeutic target in GBM.[131]

5 | CONCLUDING REMARKS

The developments and applications of MS imaging presented here highlight the immense potential of the technique for studying spatial lipid dynamics in complex biological tissues. Recent developments are increasingly overcoming significant challenges associated with sample preparation, sample throughput, and lipid identification. Moreover, standardized protocols[132,133] and data formats[134] along with round robin studies[135] and common reporting standards[136] significantly improve data reproducibility and result accuracy. This is essential to expedite the use of MSI-based applications in clinical settings.[137,138]

In summary, MALDI lipid imaging is increasingly becoming a valued technology for molecular histology significantly exceeding standard tools used to study tissue pathology. It has shown great potential for refining molecular disease pathology including neurodegenerative, neuroinflammatory, and cancer pathologies.

ACKNOWLEDGMENTS

JH is supported by the NIH (R01 AG078796, R21AG078538, R21AG080705), the Swedish Research Council VR (#2019-02397, #2023-02796), the Swedish Alzheimer Foundation (#AF-968238, #AF-939767), the Swedish Brain Foundation (Hjärnfonden, FO2022-0311), Magnus Bergvalls Stiftelse, Åhlén-Stiftelsen. (#213027), Stiftelsen Gamla Tjänarinnor and Gun och Bertil Stohnes Stiftelse. JNS is supported by the NIH (R01 AG078796, R21AG080705, R21AG072343). HZ is a Wallenberg Scholar supported by grants from the Swedish Research Council (#2023-00356, #2022-01018, and #2019-02397), the European Union's Horizon Europe research and innovation programme under grant agreement No 101053962, Swedish State Support for Clinical Research (#ALFGBG-71320), the Alzheimer Drug Discovery Foundation (ADDF), USA (#201809-2016862), the AD Strategic Fund and the Alzheimer's Association (#ADSF-21-831376-C, #ADSF-21-831381-C, and #ADSF-21-831377-C), the Bluefield Project, the Olav Thon Foundation, the Erling-Persson Family Foundation, Stiftelsen för Gamla Tjänarinnor, Hjärnfonden, Sweden (#FO2022-0270), the European Union's Horizon 2020 research and innovation programme under the Marie Skłodowska-Curie grant agreement No 860197 (MIRIADE), the European Union Joint Programme – Neurodegenerative Disease Research (JPND2021-00694), the National Institute for Health and Care Research University College London Hospitals Biomedical Research Centre, and the UK Dementia Research Institute at UCL (UKDRI-1003). KB is supported by the Swedish Research Council (#2017-00915 and #2022-00732), the Swedish Alzheimer Foundation (#AF-930351, #AF-939721, and #AF-968270), Hjärnfonden, Sweden (#FO2017-0243 and #ALZ2022-0006), the Swedish state under the agreement between the Swedish government and the County Councils, the ALF-agreement (#ALFGBG-715986 and #ALFGBG-965240), the European Union Joint Program for Neurodegenerative Disorders (JPND2019-466-236), the Alzheimer's Association 2021 Zenith Award (ZEN-21-848495), the Alzheimer's Association 2022-2025 Grant (SG-23-1038904 QC), and the Kirsten and Freddy Johansen Foundation.

CONFLICT OF INTEREST STATEMENT

HZ has served at scientific advisory boards and/or as a consultant for Abbvie, Acumen, Alector, Alzinova, ALZPath, Annexon, Apellis, Artery Therapeutics, AZTherapies, Cognito Therapeutics, CogRx, Denali, Eisai, Merry Life, Nervgen, Novo Nordisk, Optoceutics, Passage Bio, Pinteon Therapeutics, Prothena, Red Abbey Labs, reMYND, Roche, Samumed, Siemens Healthineers, Triplet Therapeutics, and Wave, has given lectures in symposia sponsored by Alzecure, Biogen, Cellectricon, Fujirebio, Lilly, and Roche, and is a co-founder of Brain Biomarker Solutions in Gothenburg AB (BBS), which is a part of the GU Ventures Incubator Program (outside submitted work). KB has served as a consultant and at advisory boards for Acumen, ALZPath, AriBio, BioArctic, Biogen, Eisai, Lilly, Moleac Pte. Ltd, Novartis, Ono Pharma, Prothena, Roche Diagnostics, and Siemens Healthineers; has served at data monitoring committees for Julius Clinical and Novartis; has given lectures, produced educational materials and participated in educational programs for AC Immune, Biogen, Celdara Medical, Eisai and Roche Diagnostics; and is a co-founder of Brain Biomarker Solutions in Gothenburg AB (BBS), which is a part of the GU Ventures Incubator Program, outside the work presented in this paper.

DATA AVAILABILITY STATEMENT

Data sharing is not applicable to this article as no new data were created or analyzed in this study.

ORCID

Jörg Hanrieder https://orcid.org/0000-0001-6059-198X

REFERENCES

1. Di Paolo G, Kim TW. Linking lipids to Alzheimer's disease: cholesterol and beyond. *Nat Rev Neurosci*. 2011;12(5):284-296. doi:10.1038/nrn3012
2. Cutler RG, Kelly J, Storie K, et al. Involvement of oxidative stress-induced abnormalities in ceramide and cholesterol metabolism in brain aging and Alzheimer's disease. *Proc Natl Acad Sci U S A*. 2004;101(7):2070-2075. doi:10.1073/pnas.0305799101

3. Belarbi K, Cuvelier E, Bonte MA, et al. Glycosphingolipids and neuroinflammation in Parkinson's disease. *Mol Neurodegener*. 2020; 15(1):59. doi:10.1186/s13024-020-00408-1
4. Leuti A, Fazio D, Fava M, Piccoli A, Oddi S, Maccarrone M. Bioactive lipids, inflammation and chronic diseases. *Adv Drug Deliv Rev*. 2020; 159:133-169. doi:10.1016/j.addr.2020.06.028
5. Bogie JFJ, Haidar M, Kooij G, Hendriks JJA. Fatty acid metabolism in the progression and resolution of CNS disorders. *Adv Drug Deliv Rev*. 2020;159:198-213. doi:10.1016/j.addr.2020.01.004
6. Gorica E, Calderone V. Arachidonic acid derivatives and neuroinflammation. *CNS Neurol Disord Drug Targets*. 2022;21(2):118-129. doi:10.2174/1871527320666210208130412
7. Fantini J, Yahi N. Molecular insights into amyloid regulation by membrane cholesterol and sphingolipids: common mechanisms in neurodegenerative diseases. *Expert Rev Mol Med*. 2010;12:e27. doi:10.1017/s1462399410001602
8. García-Viñuales S, Sciacca MFM, Lanza V, et al. The interplay between lipid and Aβ amyloid homeostasis in Alzheimer's disease: risk factors and therapeutic opportunities. *Chem Phys Lipids*. 2021; 236:105072. doi:10.1016/j.chemphyslip.2021.105072
9. Fernández-Calle R, Konings SC, Frontiñán-Rubio J, et al. APOE in the bullseye of neurodegenerative diseases: impact of the APOE genotype in Alzheimer's disease pathology and brain diseases. *Mol Neurodegener*. 2022;17(1):62. doi:10.1186/s13024-022-00566-4
10. Serrano-Pozo A, Das S, Hyman BT. APOE and Alzheimer's disease: advances in genetics, pathophysiology, and therapeutic approaches. *Lancet Neurol*. 2021;20(1):68-80. doi:10.1016/s1474-4422(20)30412-9
11. Martens YA, Zhao N, Liu CC, et al. ApoE cascade hypothesis in the pathogenesis of Alzheimer's disease and related dementias. *Neuron*. 2022;110(8):1304-1317. doi:10.1016/j.neuron.2022.03.004
12. Raulin AC, Doss SV, Trottier ZA, Ikezu TC, Bu G, Liu CC. ApoE in Alzheimer's disease: pathophysiology and therapeutic strategies. *Mol Neurodegener*. 2022;17(1):72. doi:10.1186/s13024-022-00574-4
13. Loving BA, Bruce KD. Lipid and lipoprotein metabolism in microglia. *Front Physiol*. 2020;11:393. doi:10.3389/fphys.2020.00393
14. Li RY, Qin Q, Yang HC, et al. TREM2 in the pathogenesis of AD: a lipid metabolism regulator and potential metabolic therapeutic target. *Mol Neurodegener*. 2022;17(1):40. doi:10.1186/s13024-022-00542-y
15. Guerreiro R, Wojtas A, Bras J, et al. TREM2 variants in Alzheimer's disease. *N Engl J Med*. 2013;368(2):117-127. doi:10.1056/NEJMoa1211851
16. Vance JE, Karten B. Niemann-Pick C disease and mobilization of lysosomal cholesterol by cyclodextrin. *J Lipid Res*. 2014;55(8):1609-1621. doi:10.1194/jlr.R047837
17. Breiden S, Sandhoff K. Lysosomal glycosphingolipid storage diseases *Annu Rev Biochem*. 2019;88(1):461-485. doi:10.1146/annurev-biochem-013118-111518
18. Neumann EK, Comi TJ, Spegazzini N, et al. Multimodal chemical analysis of the brain by high mass resolution mass spectrometry and infrared spectroscopic imaging. *Anal Chem*. 2018;90(19):11572-11580. doi:10.1021/acs.analchem.8b02913
19. Rabe JH, Schulz S, Munteanu B, et al. Fourier transform infrared microscopy enables guidance of automated mass spectrometry imaging to predefined tissue morphologies. *Sci Rep*. 2018;8(1):313. doi:10.1038/s41598-017-18477-6
20. Rivera ES, Djambazova KV, Neumann EK, Caprioli RM, Spraggins JM. Integrating ion mobility and imaging mass spectrometry for comprehensive analysis of biological tissues: a brief review and perspective. *J Mass Spectrom*. 2020;55(12):e4614. doi:10.1002/jms.4614
21. Kiskis J, Fink H, Nyberg L, Thyr J, Li JY, Enejder A. Plaque-associated lipids in Alzheimer's diseased brain tissue visualized by nonlinear microscopy. *Sci Rep*. 2015;5(1):13489. doi:10.1038/srep13489
22. McDonnell LA, Heeren RMA. Imaging mass spectrometry. *Mass Spectrom Rev*. 2007;26(4):606-643. doi:10.1002/mas.20124
23. Caprioli RM, Farmer TB, Gile J. Molecular imaging of biological samples: localization of peptides and proteins using MALDI-TOF MS. *Anal Chem*. 1997;69(23):4751-4760. doi:10.1021/ac970888i
24. Cornett DS, Reyzer ML, Chaurand P, Caprioli RM. MALDI imaging mass spectrometry: molecular snapshots of biochemical systems. *Nat Methods*. 2007;4(10):828-833. doi:10.1038/nmeth1094
25. Spengler, B.; Hubert, M.; Kaufmann, R. MALDI ion imaging and biological ion imaging with a new scanning UV-laser microprobe. In Proccedings of the 42nd ASMS Conference on Mass Spectrometry and Allied Topics, Chicago, Illinois, 1994.
26. Carlred L, Michno W, Kaya I, Sjovall P, Syvanen S, Hanrieder J. Probing amyloid-β pathology in transgenic Alzheimer's disease (tgArcSwe) mice using MALDI imaging mass spectrometry. *J Neurochem*. 2016;138(3):469-478. doi:10.1111/jnc.13645
27. Hanrieder J, Ljungdahl A, Falth M, Mammo SE, Bergquist J, Andersson M. L-DOPA-induced dyskinesia is associated with regional increase of striatal dynorphin peptides as elucidated by imaging mass spectrometry. *Mol Cell Proteomics*. 2011;10(10): M111.009308. doi:10.1074/mcp.M111.009308
28. Hanrieder J, Malmberg P, Ewing AG. Spatial neuroproteomics using imaging mass spectrometry. *Biochim Biophys Acta*. 2015;1854(7): 718-731. doi:10.1016/j.bbapap.2014.12.026
29. Hanrieder J, Malmberg P, Lindberg OR, Fletcher JS, Ewing AG. Time-of-flight secondary ion mass spectrometry based molecular histology of human spinal cord tissue and motor neurons. *Anal Chem*. 2013;85(18):8741-8748. doi:10.1021/ac401830m
30. Hanrieder J, Phan NT, Kurczy ME, Ewing AG. Imaging mass spectrometry in neuroscience. *ACS Chem Nerosci*. 2013;4(5):666-679. doi:10.1021/cn400053c
31. Karas M, Hillenkamp F. Laser desorption ionization of proteins with molecular masses exceeding 10000 Daltons. *Anal Chem*. 1988; 60(20):2299-2301. doi:10.1021/ac00171a028
32. Fenn JB, Mann M, Meng CK, Wong SF, Whitehouse CM. Electrospray ionization for mass-spectrometry of large biomolecules. *Science*. 1989;246(4926):64-71. doi:10.1126/science.2675315
33. Aebersold R, Mann M. Mass spectrometry-based proteomics. *Nature*. 2003;422(6928):198-207. doi:10.1038/nature01511
34. Angerer TB, Bour J, Biagi JL, Moskovets E, Frache G. Evaluation of 6 MALDI-matrices for 10 µm lipid imaging and on-tissue MSn with AP-MALDI-Orbitrap. *J Am Soc Mass Spectrom*. 2022;33(5):760-771. doi:10.1021/jasms.1c00327
35. Takats Z, Wiseman JM, Gologan B, Cooks RG. Mass spectrometry sampling under ambient conditions with desorption electrospray ionization. *Science*. 2004;306(5695):471-473. doi:10.1126/science.1104404
36. Iakab SA, Baquer G, Lafuente M, et al. SALDI-MS and SERS multimodal imaging: one nanostructured substrate to rule them both. *Anal Chem*. 2022;94(6):2785-2793. doi:10.1021/acs.analchem.1c04118
37. Northen TR, Yanes O, Northen MT, et al. Clathrate nanostructures for mass spectrometry. *Nature*. 2007;449(7165):1033-1036. doi:10.1038/nature06195
38. Vickerman JC. Molecular imaging and depth profiling by mass spectrometry—SIMS, MALDI or DESI? *Analyst*. 2011;136(11):2199-2217. doi:10.1039/c1an00008j
39. Passarelli MK, Winograd N, Lipid imaging with time-of-flight secondary ion mass spectrometry (ToF-SIMS) *Biochim Biophys Acta Mol Cell Biol Lipids*.. 2011;1811(11):976-990. doi:10.1016/j.bbalip.2011.05.007
40. Steinhauser M, Bailey A, Senyo S, et al. Multi-isotope imaging mass spectrometry quantifies stem cell division and metabolism *Nature*. 2012;481:516-519. doi:10.1038/nature10734

41. Coskun AF, Han G, Ganesh S, et al. Nanoscopic subcellular imaging enabled by ion beam tomography. *Nat Commun*. 2021;12:789. doi:10.1038/s41467-020-20753-5
42. Wehrli PM, Ge J, Michno W, et al. Correlative chemical imaging and spatial chemometrics delineate Alzheimer plaque heterogeneity at high spatial resolution. *JACS au*. 2023;3(3):762-774. doi:10.1021/jacsau.2c00492
43. Kompauer M, Heiles S, Spengler B. Atmospheric pressure MALDI mass spectrometry imaging of tissues and cells at 1.4-mum lateral resolution. *Nat Methods*. 2017;14(1):90-96. doi:10.1038/nmeth.4071
44. Niehaus M, Soltwisch J, Belov ME, Dreisewerd K. Transmission-mode MALDI-2 mass spectrometry imaging of cells and tissues at subcellular resolution. *Nat Methods*. 2019;16(9):925-931. doi:10.1038/s41592-019-0536-2
45. Goodwin RJA, Dungworth JC, Cobb SR, Pitt AR. Time-dependent evolution of tissue markers by MALDI-MS imaging. *Proteomics*. 2008;8(18):3801-3808. doi:10.1002/pmic.200800201
46. Patterson NH, Thomas A, Chaurand P. Monitoring time-dependent degradation of phospholipids in sectioned tissues by MALDI imaging mass spectrometry. *J Mass Spectrom*. 2014;49(7):622-627. doi:10.1002/jms.3382
47. Hanrieder J, Ljungdahl A, Andersson M. MALDI imaging mass spectrometry of neuropeptides in Parkinson's disease. *J vis Exp*. 2012;60:e3445. doi:10.3791/3445
48. Angel PM, Spraggins JM, Baldwin HS, Caprioli R. Enhanced sensitivity for high spatial resolution lipid analysis by negative ion mode matrix assisted laser desorption ionization imaging mass spectrometry. *Anal Chem*. 2012;84(3):1557-1564. doi:10.1021/ac202383m
49. Wang HY, Liu CB, Wu HW. A simple desalting method for direct MALDI mass spectrometry profiling of tissue lipids. *J Lipid Res*. 2011;52(4):840-849. doi:10.1194/jlr.D013060
50. Seeley EH, Oppenheimer SR, Mi D, Chaurand P, Caprioli RM. Enhancement of protein sensitivity for MALDI imaging mass spectrometry after chemical treatment of tissue sections. *J Am Soc Mass Spectrom*. 2008;19(8):1069-1077. doi:10.1016/j.jasms.2008.03.016
51. Thomas A, Patterson NH, Laveaux Charbonneau J, Chaurand P. Orthogonal organic and aqueous-based washes of tissue sections to enhance protein sensitivity by MALDI imaging mass spectrometry. *J Mass Spectrom*. 2013;48(1):42-48. doi:10.1002/jms.3114
52. Wei J, Buriak JM, Siuzdak G. Desorption-ionization mass spectrometry on porous silicon. *Nature*. 1999;399(6733):243-246. doi:10.1038/20400
53. Fincher JA, Dyer JE, Korte AR, Yadavilli S, Morris NJ, Vertes A. Matrix-free mass spectrometry imaging of mouse brain tissue sections on silicon nanopost arrays. *J Comp Neurol*. 2019;527(13):2101-2121. doi:10.1002/cne.24566
54. Stopka SA, Rong C, Korte AR, et al. Molecular imaging of biological samples on nanophotonic laser desorption ionization platforms. *Angew Chem Int Ed Engl*. 2016;55(14):4482-4486. doi:10.1002/anie.201511691
55. Puolitaival SM, Burnum KE, Cornett DS, Caprioli RM. Solvent-free matrix dry-coating for MALDI imaging of phospholipids. *J Am Soc Mass Spectrom*. 2008;19(6):882-886. doi:10.1016/j.jasms.2008.02.013
56. Thomas A, Charbonneau JL, Fournaise E, Chaurand P. Sublimation of new matrix candidates for high spatial resolution imaging mass spectrometry of lipids: enhanced information in both positive and negative polarities after 1,5-diaminonapthalene deposition. *Anal Chem*. 2012;84(4):2048-2054. doi:10.1021/ac2033547
57. Yang J, Caprioli RM. Matrix sublimation/recrystallization for imaging proteins by mass spectrometry at high spatial resolution. *Anal Chem*. 2011;83(14):5728-5734. doi:10.1021/ac200998a
58. Hankin JA, Barkley RM, Murphy RC. Sublimation as a method of matrix application for mass spectrometric imaging. *J Am Soc Mass Spectrom*. 2007;18(9):1646-1652. doi:10.1016/j.jasms.2007.06.010
59. Dufresne M, Patterson NH, Norris JL, Caprioli RM. Combining salt doping and matrix sublimation for high spatial resolution MALDI imaging mass spectrometry of neutral lipids. *Anal Chem*. 2019;91(20):12928-12934. doi:10.1021/acs.analchem.9b02974
60. Schiller J, Süss R, Fuchs B, et al. The suitability of different DHB isomers as matrices for the MALDI-TOF MS analysis of phospholipids: which isomer for what purpose? *Eur Biophys J*. 2007;36(4–5):517-527. doi:10.1007/s00249-006-0090-6
61. Scott AJ, Flinders B, Cappell J, et al. Norharmane matrix enhances detection of endotoxin by MALDI-MS for simultaneous profiling of pathogen, host, and vector systems. *Pathog Dis*. 2016;74(8):ftw097. doi:10.1093/femspd/ftw097
62. Cheng H, Sun G, Yang K, Gross RW, Han X. Selective desorption/ionization of sulfatides by MALDI-MS facilitated using 9-aminoacridine as matrix. *J Lipid Res*. 2010;51(6):1599-1609. doi:10.1194/jlr.D004077
63. Wang J, Qiu S, Chen S, et al. MALDI-TOF MS imaging of metabolites with a N-(1-naphthyl) ethylenediamine dihydrochloride matrix and its application to colorectal cancer liver metastasis. *Anal Chem*. 2015;87(1):422-430. doi:10.1021/ac504294s
64. Shimma S, Sugiura Y, Hayasaka T, Zaima N, Matsumoto M, Setou M. Mass imaging and identification of biomolecules with MALDI-QIT-TOF-based system. *Anal Chem*. 2008;80(3):878-885. doi:10.1021/ac071301v
65. Nishiguchi M, Ueno Y, Toyoda M, Setou M. Design of a new multi-turn ion optical system 'IRIS' for a time-of-flight mass spectrometer. *J Mass Spectrom*. 2009;44(5):594-604. doi:10.1002/jms.1531
66. Toyoda M, Ishihara M, Yamaguchi S, et al. Construction of a new multi-turn time-of-flight mass spectrometer. *J Mass Spectrom*. 2000;35(2):163-167. doi:10.1002/(sici)1096-9888(200002)35:23.0.Co;2-g
67. Vestal M, Li L, Dobrinskikh E, et al. Rapid MALDI-TOF molecular imaging: instrument enhancements and their practical consequences. *J Mass Spectrom*. 2020;55(8):e4423. doi:10.1002/jms.4423
68. Islam A, Sakamoto T, Zhai Q, et al. Application of AP-MALDI imaging mass microscope for the rapid mapping of imipramine, chloroquine, and their metabolites in the kidney and brain of wild-type mice. *Pharmaceuticals (Basel)*. 2022;15(11):1314. doi:10.3390/ph15111314
69. Rompp A, Guenther S, Schober Y, et al. Histology by mass spectrometry: label-free tissue characterization obtained from high-accuracy bioanalytical imaging. *Angew Chem Int Ed Engl*. 2010;49(22):3834-3838. doi:10.1002/anie.200905559
70. Jackson SN, Ugarov M, Egan T, et al. MALDI-ion mobility-TOFMS imaging of lipids in rat brain tissue. *J Mass Spectrom*. 2007;42(8):1093-1098. doi:10.1002/jms.1245
71. Lamont L, Hadavi D, Bowman AP, et al. High-resolution ion mobility spectrometry-mass spectrometry for isomeric separation of prostanoids after Girard's reagent T derivatization. *Rapid Commun Mass Spectrom*. 2023;37(5):e9439. doi:10.1002/rcm.9439
72. Michno W, Wehrli PM, Koutarapu S, et al. Structural amyloid plaque polymorphism is associated with distinct lipid accumulations revealed by trapped ion mobility mass spectrometry imaging. *J Neurochem*. 2022;160(4):482-498. doi:10.1111/jnc.15557
73. Qian Y, Guo X, Wang Y, Ouyang Z, Ma X. Mobility-modulated sequential dissociation analysis enables structural lipidomics in mass spectrometry imaging. *Angew Chem Int Ed Engl*. 2023;62(52):e202312275. doi:10.1002/anie.202312275
74. Kaya I, Michno W, Brinet D, et al. Histology-compatible MALDI mass spectrometry based imaging of neuronal lipids for subsequent immunofluorescent staining. *Anal Chem*. 2017;89(8):4685-4694. doi:10.1021/acs.analchem.7b00313

75. O'Rourke MB, Smith CC, De La Monte SM, Sutherland GT, Padula MP. Higher mass accuracy MALDI-TOF/TOF lipid imaging of human brain tissue in Alzheimer's disease. *Curr Protoc Mol Biol*. 2019;126(1):e86. doi:10.1002/cpmb.86
76. Kaya I, Nilsson A, Luptakova D, et al. Spatial lipidomics reveals brain region-specific changes of sulfatides in an experimental MPTP Parkinson's disease primate model. *NPJ Parkinsons Dis*. 2023;9(1):118. doi:10.1038/s41531-023-00558-1
77. Tobias F, Olson MT, Cologna SM. Mass spectrometry imaging of lipids: untargeted consensus spectra reveal spatial distributions in Niemann-Pick disease type C1. *J Lipid Res*. 2018;59(12):2446-2455. doi:10.1194/jlr.D086090
78. Prentice BM, Chumbley CW, Caprioli RM. High-speed MALDI MS/MS imaging mass spectrometry using continuous raster sampling. *J Mass Spectrom*. 2015;50(4):703-710. doi:10.1002/jms.3579
79. Kaya I, Jennische E, Lange S, Tarik Baykal A, Malmberg P, Fletcher JS. Brain region-specific amyloid plaque-associated myelin lipid loss, APOE deposition and disruption of the myelin sheath in familial Alzheimer's disease mice. *J Neurochem*. 2020;154(1):84-98. doi:10.1111/jnc.14999
80. Mallah K, Quanico J, Raffo-Romero A, et al. Matrix-assisted laser desorption/ionization-mass spectrometry imaging of lipids in experimental model of traumatic brain injury detecting acylcarnitines as injury related markers. *Anal Chem*. 2019;91(18):11879-11887. doi:10.1021/acs.analchem.9b02633
81. Liang X, Cao S, Xie P, et al. Three-dimensional imaging of whole-body zebrafish revealed lipid disorders associated with Niemann-Pick disease type C1. *Anal Chem*. 2021;93(23):8178-8187. doi:10.1021/acs.analchem.1c00196
82. Jackson SN, Wang HY, Woods AS. In situ structural characterization of phosphatidylcholines in brain tissue using MALDI-MS/MS. *J Am Soc Mass Spectrom*. 2005;16(12):2052-2056. doi:10.1016/j.jasms.2005.08.014
83. Angelini R, Yutuc E, Wyatt MF, et al. Visualizing cholesterol in the brain by on-tissue derivatization and quantitative mass spectrometry imaging. *Anal Chem*. 2021;93(11):4932-4943. doi:10.1021/acs.analchem.0c05399
84. Kaya I, Jennische E, Dunevall J, et al. Spatial lipidomics reveals region and long chain base specific accumulations of monosialoganglioside in amyloid plaques in familial Alzheimer's disease mice (5xFAD) brain. *ACS Chem Nerosci*. 2020;11(1):14-24. doi:10.1021/acschemneuro.9b00532
85. Tortorella S, Tiberi P, Bowman AP, et al. LipostarMSI: comprehensive, vendor-neutral software for visualization, data analysis, and automated molecular identification in mass spectrometry imaging. *J Am Soc Mass Spectrom*. 2020;31(1):155-163. doi:10.1021/jasms.9b00034
86. Robichaud G, Garrard KP, Barry JA, Muddiman DC. MSiReader: an open-source interface to view and analyze high resolving power MS imaging files on Matlab platform. *J Am Soc Mass Spectrom*. 2013;24(5):718-721. doi:10.1007/s13361-013-0607-z
87. Bemis KD, Harry A, Eberlin LS, et al. Cardinal: an R package for statistical analysis of mass spectrometry-based imaging experiments. *Bioinformatics*. 2015;31(14):2418-2420. doi:10.1093/bioinformatics/btv146
88. Rauch MAMS. Biomap 2000, https://ms-imaging.org/wp/biomap/
89. Källback P, Nilsson A, Shariatgorji M, Andrén PE. msIQuant—quantitation software for mass spectrometry imaging enabling fast access, visualization, and analysis of large data sets. *Anal Chem*. 2016;88(8):4346-4353. doi:10.1021/acs.analchem.5b04603
90. Race AM, Palmer AD, Dexter A, Steven RT, Styles IB, Bunch J. SpectralAnalysis: software for the masses. *Anal Chem*. 2016;88(19):9451-9458. doi:10.1021/acs.analchem.6b01643
91. Wehrli PM, Michno W, Blennow K, Zetterberg H, Hanrieder J. Chemometric strategies for sensitive annotation and validation of anatomical regions of interest in complex imaging mass spectrometry data. *J Am Soc Mass Spectrom*. 2019;30(11):2278-2288. doi:10.1007/s13361-019-02327-y
92. Deininger S-O, Ebert MP, Fuetterer A, Gerhard M, Roecken C. MALDI imaging combined with hierarchical clustering as a new tool for the interpretation of complex human cancers. *J Proteome Res*. 2008;7(12):5230-5236. doi:10.1021/pr8005777
93. Palmer A, Phapale P, Chernyavsky I, et al. FDR-controlled metabolite annotation for high-resolution imaging mass spectrometry. *Nat Methods*. 2017;14(1):57-60. doi:10.1038/nmeth.4072
94. Aimo L, Liechti R, Hyka-Nouspikel N, et al. The SwissLipids knowledgebase for lipid biology. *Bioinformatics*. 2015;31(17):2860-2866. doi:10.1093/bioinformatics/btv285
95. Sud M, Fahy E, Cotter D, et al. LMSD: LIPID MAPS structure database. *Nucleic Acids Res*. 2007;35:D527-D532. doi:10.1093/nar/gkl838
96. Fahy E, Subramaniam S, Murphy RC, et al. Update of the LIPID MAPS comprehensive classification system for lipids. *J Lipid Res*. 2009;50(Suppl):S9-S14. doi:10.1194/jlr.R800095-JLR200
97. Porta Siegel T, Ekroos K, Ellis SR. Reshaping lipid biochemistry by pushing barriers in structural lipidomics. *Angew Chem Int Ed Engl*. 2019;58(20):6492-6501. doi:10.1002/anie.201812698
98. Thomas MC, Mitchell TW, Harman DG, Deeley JM, Murphy RC, Blanksby SJ. Elucidation of double bond position in unsaturated lipids by ozone electrospray ionization mass spectrometry. *Anal Chem*. 2007;79(13):5013-5022. doi:10.1021/ac0702185
99. Bednařík A, Bölsker S, Soltwisch J, Dreisewerd K. An on-tissue Paternò-Büchi reaction for localization of carbon-carbon double bonds in phospholipids and glycolipids by matrix-assisted laser-desorption-ionization mass-spectrometry imaging. *Angew Chem Int Ed Engl*. 2018;57(37):12092-12096. doi:10.1002/anie.201806635
100. Su Y, Ma X, Page J, Shi R, Xia Y, Ouyang Z. Mapping lipid C=C location isomers in organ tissues by coupling photochemical derivatization and rapid extractive mass spectrometry. *Int J Mass Spectrom*. 2019;445:116206. doi:10.1016/j.ijms.2019.116206
101. Wäldchen F, Spengler B, Heiles S. Reactive matrix-assisted laser desorption/ionization mass spectrometry imaging using an intrinsically photoreactive Paternò-Büchi matrix for double-bond localization in isomeric phospholipids. *J Am Chem Soc*. 2019;141(30):11816-11820. doi:10.1021/jacs.9b05868
102. Paine MRL, Poad BLJ, Eijkel GB, et al. Mass spectrometry imaging with isomeric resolution enabled by ozone-induced dissociation. *Angew Chem Int Ed Engl*. 2018;57(33):10530-10534. doi:10.1002/anie.201802937
103. Yang E, Dufresne M, Chaurand P. Enhancing ganglioside species detection for MALDI-TOF imaging mass spectrometry in negative reflectron mode. *Int J Mass Spectr*. 2019;437:3-9. doi:10.1016/j.ijms.2017.09.011
104. Kaya I, Brinet D, Michno W, et al. Delineating amyloid plaque associated neuronal sphingolipids in transgenic Alzheimer's disease mice (tgArcSwe) using MALDI imaging mass spectrometry. *ACS Chem Nerosci*. 2017;8(2):347-355. doi:10.1021/acschemneuro.6b00391
105. Hong JH, Kang JW, Kim DK, et al. Global changes of phospholipids identified by MALDI imaging mass spectrometry in a mouse model of Alzheimer's disease. *J Lipid Res*. 2016;57(1):36-45. doi:10.1194/jlr.M057869
106. Caughlin S, Maheshwari S, Agca Y, et al. Membrane-lipid homeostasis in a prodromal rat model of Alzheimer's disease: characteristic profiles in ganglioside distributions during aging detected using MALDI imaging mass spectrometry. *Biochim Biophys Acta Gen Subj*. 2018;1862(6):1327-1338. doi:10.1016/j.bbagen.2018.03.011
107. Michno W, Kaya I, Nystrom S, et al. Multimodal chemical imaging of amyloid plaque polymorphism reveals Aβ aggregation dependent anionic lipid accumulations and metabolism. *Anal Chem*. 2018;90(13):8130-8138. doi:10.1021/acs.analchem.8b01361

108. Michno W, Wehrli PM, Zetterberg H, Blennow K, Hanrieder J. GM1 locates to mature amyloid structures implicating a prominent role for glycolipid-protein interactions in Alzheimer pathology. *Biochim Biophys Acta Proteins Proteomics*. 2019;1867(5):458-467. doi:10.1016/j.bbapap.2018.09.010
109. Kaya I, Brinet D, Michno W, et al. Novel trimodal MALDI imaging mass spectrometry (IMS3) at 10 μm reveals spatial lipid and peptide correlates implicated in Aβ plaque pathology in Alzheimer's disease. *ACS Chem Neurosci*. 2017;8(12):2778-2790. doi:10.1021/acschemneuro.7b00314
110. Kaya I, Zetterberg H, Blennow K, Hanrieder J. Shedding light on the molecular pathology of amyloid plaques in transgenic Alzheimer's disease mice using multimodal MALDI imaging mass spectrometry. *ACS Chem Neurosci*. 2018;9(7):1802-1817. doi:10.1021/acschemneuro.8b00121
111. Michno W, Nystrom S, Wehrli P, et al. Pyroglutamation of amyloid-βx-42 (Aβx-42) followed by Aβ1-40 deposition underlies plaque polymorphism in progressing Alzheimer's disease pathology. *J Biol Chem*. 2019;294(17):6719-6732. doi:10.1074/jbc.RA118.006604
112. Michno W, Bowman A, Jha D, et al. Chemical imaging of sphingolipids and phospholipids at the single amyloid-β plaque level in post-mortem human Alzheimer's disease brain. ChemRxiv, 2023.
113. Arima H, Omura T, Hayasaka T, et al. Reductions of docosahexaenoic acid-containing phosphatidylcholine levels in the anterior horn of an ALS mouse model. *Neuroscience*. 2015;297:127-136. doi:10.1016/j.neuroscience.2015.03.060
114. Jang HJ, Le MUT, Park JH, et al. Matrix-assisted laser desorption/ionization mass spectrometry imaging of phospholipid changes in a drosophila model of early amyotrophic lateral sclerosis. *J Am Soc Mass Spectrom*. 2021;32(10):2536-2545. doi:10.1021/jasms.1c00167
115. Skold K, Svensson M, Nilsson A, et al. Decreased striatal levels of PEP-19 following MPTP lesion in the mouse. *J Proteome Res*. 2006;5(2):262-269. doi:10.1021/pr050281f
116. Ungerstedt U. 6-Hydroxy-dopamine induced degeneration of central monoamine neurons. *Eur J Pharmacol*. 1968;5(1):107-110. doi:10.1016/0014-2999(68)90164-7
117. Tobias F, Pathmasiri KC, Cologna SM. Mass spectrometry imaging reveals ganglioside and ceramide localization patterns during cerebellar degeneration in the Npc1(−/−) mouse model. *Anal Bioanal Chem*. 2019;411(22):5659-5668. doi:10.1007/s00216-019-01989-7
118. Barre FPY, Paine MRL, Flinders B, et al. Enhanced sensitivity using MALDI imaging coupled with laser postionization (MALDI-2) for pharmaceutical research. *Anal Chem*. 2019;91(16):10840-10848. doi:10.1021/acs.analchem.9b02495
119. Dufresne M, Thomas A, Breault-Turcot J, Masson JF, Chaurand P. Silver-assisted laser desorption ionization for high spatial resolution imaging mass spectrometry of olefins from thin tissue sections. *Anal Chem*. 2013;85(6):3318-3324. doi:10.1021/ac3037415
120. Patti GJ, Shriver LP, Wassif CA, et al. Nanostructure-initiator mass spectrometry (NIMS) imaging of brain cholesterol metabolites in Smith-Lemli-Opitz syndrome. *Neuroscience*. 2010;170(3):858-864. doi:10.1016/j.neuroscience.2010.07.038
121. Cobice DF, Mackay CL, Goodwin RJ, et al. Mass spectrometry imaging for dissecting steroid intracrinology within target tissues. *Anal Chem*. 2013;85(23):11576-11584. doi:10.1021/ac402777k
122. Muller L, Baldwin K, Barbacci DC, et al. Laser desorption/ionization mass spectrometric imaging of endogenous lipids from rat brain tissue implanted with silver nanoparticles. *J Am Soc Mass Spectrom*. 2017;28(8):1716-1728. doi:10.1007/s13361-017-1665-4
123. Nezhad ZS, Salazar JP, Pryce RS, Munter LM, Chaurand P. Absolute quantification of cholesterol from thin tissue sections by silver-assisted laser desorption ionization mass spectrometry imaging. *Anal Bioanal Chem*. 2022;414(23):6947-6954. doi:10.1007/s00216-022-04262-6
124. Ermini L, Morganti E, Post A, et al. Imaging mass spectrometry identifies prognostic ganglioside species in rodent intracranial transplants of glioma and medulloblastoma. *PLoS ONE*. 2017;12(5):e0176254. doi:10.1371/journal.pone.0176254
125. Clark AR, Calligaris D, Regan MS, et al. Rapid discrimination of pediatric brain tumors by mass spectrometry imaging. *J Neurooncol*. 2018;140(2):269-279. doi:10.1007/s11060-018-2978-2
126. Paine MRL, Liu J, Huang D, et al. Three-dimensional mass spectrometry imaging identifies lipid markers of medulloblastoma metastasis. *Sci Rep*. 2019;9(1):2205. doi:10.1038/s41598-018-38257-0
127. Kampa JM, Kellner U, Marsching C, et al. Glioblastoma multiforme: metabolic differences to peritumoral tissue and IDH-mutated gliomas revealed by mass spectrometry imaging. *Neuropathology*. 2020;40(6):546-558. doi:10.1111/neup.12671
128. Dilillo M, Ait-Belkacem R, Esteve C, et al. Ultra-high mass resolution MALDI imaging mass spectrometry of proteins and metabolites in a mouse model of glioblastoma. *Sci Rep*. 2017;7(1):603. doi:10.1038/s41598-017-00703-w
129. Wang HJ, Huang CY, Wei KC, Hung KC. A mass spectrometry imaging and lipidomic investigation reveals aberrant lipid metabolism in the orthotopic mouse glioma. *J Lipid Res*. 2022;63(12):100304. doi:10.1016/j.jlr.2022.100304
130. Abdelmoula WM, Lopez BG, Randall EC, et al. Peak learning of mass spectrometry imaging data using artificial neural networks. *Nat Commun*. 2021;12(1):5544. doi:10.1038/s41467-021-25744-8
131. Schwaiger-Haber M, Stancliffe E, Anbukumar DS, et al. Using mass spectrometry imaging to map fluxes quantitatively in the tumor ecosystem. *Nat Commun*. 2023;14(1):2876. doi:10.1038/s41467-023-38403-x
132. Lamont L, Hadavi D, Viehmann B, et al. Quantitative mass spectrometry imaging of drugs and metabolites: a multiplatform comparison. *Anal Bioanal Chem*. 2021;413(10):2779-2791. doi:10.1007/s00216-021-03210-0
133. Balluff B, Hopf C, Porta Siegel T, Grabsch HI, Heeren RMA. Batch effects in MALDI mass spectrometry imaging. *J Am Soc Mass Spectrom*. 2021;32(3):628-635. doi:10.1021/jasms.0c00393
134. Schramm T, Hester Z, Klinkert I, et al. imzML—a common data format for the flexible exchange and processing of mass spectrometry imaging data. *J Proteomics*. 2012;75(16):5106-5110. doi:10.1016/j.jprot.2012.07.026
135. Buck A, Heijs B, Beine B, et al. Round robin study of formalin-fixed paraffin-embedded tissues in mass spectrometry imaging. *Anal Bioanal Chem*. 2018;410(23):5969-5980. doi:10.1007/s00216-018-1216-2
136. McDonnell LA, Rompp A, Balluff B, et al. Discussion point: reporting guidelines for mass spectrometry imaging. *Anal Bioanal Chem*. 2015;407(8):2035-2045. doi:10.1007/s00216-014-8322-6
137. Spraggins JM, Schwamborn K, Heeren RMA, Eberlin LS. The importance of clinical tissue imaging. *Clin Mass Spectrom*. 2019;12:47-49. doi:10.1016/j.clinms.2019.04.001
138. Leung F, Eberlin LS, Schwamborn K, Heeren RMA, Winograd N, Cooks RG. Mass spectrometry-based tissue imaging: the next frontier in clinical diagnostics? *Clin Chem*. 2019;65(4):510-513. doi:10.1373/clinchem.2018.289694

How to cite this article: Jha D, Blennow K, Zetterberg H, Savas JN, Hanrieder J. Spatial neurolipidomics—MALDI mass spectrometry imaging of lipids in brain pathologies. *J Mass Spectrom*. 2024;59(3):e5008. doi:10.1002/jms.5008